Single-channel, macroscopic, and gating currents from sodium channels in the squid giant axon

C. A. Vandenberg* and F. Bezanilla‡

*Department of Biological Sciences and Neurosciences Research Institute, University of California, Santa Barbara, California 93106; and ‡Department of Physiology, Ahmanson Laboratory of Neurobiology and Jerry Lewis Neuromuscular Research Center, University of California, Los Angeles, California 90024

ABSTRACT Single-channel, macroscopic ionic, and macroscopic gating currents were recorded from the voltage-dependent sodium channel using patch-clamp techniques on the cut-open squid giant axon. To obtain a complete set of physiological measurements of sodium channel gating under identical conditions, and to facilitate comparison with previous work, comparison was made between currents recorded in the absence of extracellular divalent cations and in the presence of physiological concentrations of extracellular Ca^{2+} (10 mM) and Mg^{2+} (50 mM). The single-channel currents were well resolved when divalent cations were not included in the extracellular solution, but were decreased in amplitude in the presence of Ca^{2+} and Mg^{2+} ions. The instantaneous current-voltage relationship obtained from macroscopic tail current measurements similarly was depressed by divalents, and showed a negative slope-conductance region for inward current at negative potentials. Voltage dependent parameters of channel gating were shifted 9–13 mV towards depolarized potentials by external divalent cations, including the peak fraction of channels open versus voltage, the time constant of tail current decline, the prepulse inactivation versus voltage relationship, and the charge-voltage relationship for gating currents. The effects of divalent cations are consistent with open channel block by Ca^{2+} and Mg^{2+} together with divalent screening of membrane charges.

INTRODUCTION

The generation and propagation of the nerve impulse is the result of sodium and potassium conductance changes in the nerve membrane, as described by Hodgkin and Huxley (1952*a*) in their classical study of the voltage-clamped currents of the squid giant axon. A goal in the understanding of the voltage-dependent sodium conductance has been a description of the mechanism of channel gating. Models of channel gating have been proposed based on various measurements of channel function, such as macroscopic ionic currents, single-channel currents, and gating currents. However, it has not been possible to take advantage of these different manifestations of channel function to produce a consistent gating model of the channel in its native membrane because data were collected from different preparations and under different conditions. With the introduction of the cut-open axon technique, that allows one to perform patch clamp experiments from the internal face of the axonal membrane (Bezanilla, 1987; Llano et al., 1988; Bezanilla and Vandenberg, 1990) it is feasible finally to record all the electrical expressions of sodium channel gating from the squid axon, where most of the classical studies on sodium channels have been made.

This paper and the following one (Vandenberg and Bezanilla, 1991) are a detailed study of the characteristics of the sodium channel in the squid giant axon at the single channel level, and at the level of macroscopic ionic currents and gating currents. The main concern in these papers is on the mechanisms of voltage dependent gating of the sodium channel, with some emphasis given to the conduction properties of the open channel. The first paper presents the results on patch recordings of macroscopic and gating currents with a comparison to the results in whole axons, whereas the second paper concentrates on single channel recording and modeling of the sodium channel gating based on single channel, macroscopic and gating current data.

In this study, we show that sodium single-channel, macroscopic ionic and gating currents can be recorded reliably from the cut-open axon in the absence of divalent cations in the external solution. For comparison to results in whole axons, we evaluated the effect of divalent cations on the gating and permeation characteristics of the sodium channel. Our observations indicate that Ca^{2+} and Mg^{2+} affect both the channel conductance, due to voltage-dependent block, and the channel gating, due to charge screening. Accounts of some of these results have been presented previously in abstract form (Vandenberg and Bezanilla, 1988, 1990).

METHODS

Axon preparation

All the experiments reported here have been performed in segments of the giant axon of the squid *Loligo pealei* obtained at the Marine

Address corredpondence to Dr. Vandenberg.

0006-3495/91/12/1499/12 $2.00

Biological Laboratory in Woods Hole, MA. Axons were dissected from the squid mantle in running sea water and then cleaned of other nerve fibers and connective tissue under a dissecting microscope.

Most of the experiments were done using the cut-open axon technique that has been described previously (Llano et al., 1988; Bezanilla and Vandenberg, 1990). Briefly, a segment of axon of about 7 mm in length was tied at both ends and pinned to the bottom of a Sylgard-coated chamber. The experimental chamber was a narrow (5 mm wide × 20 mm long) rectangular dish of Lucite and glass that permitted solution around the preparation to be exchanged readily by flowing it from one end of the chamber to the other along the length of the axon. The axon segment was cut open longitudinally with microscissors in artificial sea water (50 Mg, 10 Ca ASW; see Table 1 for solution compositions). After 2–5 min, the solution was changed to 546 Na by exchanging 10–20 bath volumes of the solution across the cut-open axon, and removing the axoplasm with suction. Because the cut-open axon was pinned loosely to the bottom of the chamber, solution exchange was rapid and complete on both sides of the axonal membrane. This procedure cleaned away the axoplasm and allowed the approach of patch pipettes to the inside surface of the axon. All the patches were of the outside-out type (Hamill et al., 1981) formed by making a gigaseal on the intracellular surface of the axonal membrane with the patch pipette. Patch pipettes were fabricated from Corning 7040 or 7052 glass (Garner Glass Co., Claremont, CA), coated with Sylgard 184 (Dow-Corning Corp., Midland, MI), and had resistances in the recording solution of 1–4 MΩ.

Some experiments were performed with internally dialyzed whole axons (Brinley and Mullins, 1967) that were voltage clamped with axial wire and internal electrodes according to the methods described by DiPolo et al. (1985). In this technique, the axial wire for passing current was positioned inside the dialysis capillary which was inserted from one end of the axon while the internal voltage-measuring electrode was inserted from the other end of the axon.

All experiments were performed at 5°C.

Data acquisition

Patch clamp experiments were performed using a List EPC7 patch clamp (Medical Systems Corp., Greenvale, NY), and voltage clamp experiments from dialyzed axons were done with a voltage clamp similar to that described previously (Bezanilla and Armstrong, 1977; Bezanilla, et al., 1982). Currents were low pass filtered with a four or eight pole Bessel filter and digitized with a data acquisition system built around an IBM AT-compatible computer that is similar to the one described by Stimers et al. (1987). Digital data were stored on magnetic media or optical disk for off-line analysis. The pattern of voltage pulses applied was controlled by the acquisition program. Pulses were generated by a dedicated waveform generator that was memory mapped in the computer as described previously (Stimers et al., 1987).

Macroscopic ionic currents and gating currents were corrected for linear leakage and capacitative currents with the P/−4 procedure (Bezanilla and Armstrong, 1977) from a subtracting holding potential of −118 mV, unless indicated otherwise. Signal averaging was used to improve the signal-to-noise ratio for macroscopic currents, as indicated in the figure legends.

Data analysis

Theoretical curves were fitted to the data using nonlinear least-squares regression based on the Marquardt-Levenberg algorithm. Many of the data sets, as indicated in the text, were fitted with a simple voltage-dependent process described by the Boltzmann distribution:

$$Y = 1/[1 + \exp[(zF/RT)(V_{1/2} - V)]], \quad (1)$$

where F, R, and T have their usual meaning. V is the membrane voltage, $V_{1/2}$ is the midpoint of the curve along the voltage axis, and z is the effective valence of the process, giving the steepness of the curve. Shifts in the curves under different ionic conditions are reported as the differences in the $V_{1/2}$ values.

Solutions and conventions

The composition of the solutions used is detailed in Table 1. The convention followed in the text is external//internal solution. All the potentials reported here were corrected for liquid junction potentials. Measured liquid junction potentials ranged between 3 and 10 mV for the various combinations of solutions used, and were reproducibly within 0.5 mV for measurements of the same pairs of solutions.

TABLE 1 Recording Solutions

	Na	Mg	Ca	Cs	NMG*	Tris‡	TEA§	Cl	F	Glutamate	EGTA	HEPES	Sucrose
External solutions													
546 Na	546	—	—	—	—	—	—	540	—	—	—	10	—
10 Ca ASW	536	—	10	—	—	—	—	550	—	—	—	10	—
50 Mg, 10 Ca ASW	446	50	10	—	—	—	—	560	—	—	—	10	—
10% ASW	44	5	1	209	270	—	—	529	—	—	—	10	—
Patch Gating	—	—	—	231	300	—	—	525	—	—	—	10	—
1 Ca Gating‖	—	—	1	—	—	588	—	449	—	—	—	—	—
4 Ca Gating‖	—	—	4	—	—	583	—	451	—	—	—	—	—
50 Mg, 10 Ca Gating‖	—	50	10	—	—	494	—	495	—	—	—	—	—
Internal solutions													
Patch Ionic	50	—	—	159	—	—	—	10	20	165	5	10	460
Patch Gating	—	—	—	159	—	—	50	10	20	165	5	10	460
Dialysis Ionic & Gating¶	—	—	—	—	145	10	50	—	140	50	5	10	470

All solutions had an osmolality of 1,000 mosmol/kg. The external solutions were pH 7.6, and internal solutions were pH 7.3. Concentrations are in millimolar. *N-methyl-D-glucamine; ‡Tris(hydroxymethyl)aminomethane; §Tetraethylammonium; ‖300 nM tetrodotoxin was also included in these solutions; and ¶in some experiments tetramethylammonium was substituted for NMG.

RESULTS

Macroscopic sodium currents

The use of large patch pipettes (2–8 μm in diameter) allowed us to record macroscopic sodium currents of up to 2.5 nA peak current from the cut-open axon. Data used in the analysis had a maximum of 0.7 nA current. Although the density of current was much higher than was obtained with smaller patches, the number of channels was variable, and sometimes there were only a few channels in large patches. Conversely, we sometimes found a large number of channels in small patches, indicating that the distribution of channels is not uniform. The density of channels did not appear to correlate with surface features such as the location of axonal branches, but multiple patches formed in a region of high channel density usually gave similar channel density. The patches with large pipettes lasted for shorter times than patches formed using small pipettes, but we frequently obtained stable large patches that allowed us to record macroscopic ionic or gating currents for about an hour.

Fig. 1 shows a family of sodium currents recorded for a series of depolarizations from −48 to +82 mV in increments of 10 mV from a holding potential of −108 mV. In *A* of Fig. 1 the external solution was artificial seawater (50 Mg, 10 Ca ASW) and in *B*, the currents were recorded in 546 Na which contained no added divalent cations. The time courses of the currents under both recording conditions were similar, except that the voltage dependence of the kinetics was shifted to the left along the voltage axis for the recordings made in the absence of divalents. The currents recorded in the absence of divalents also tended to be larger than with divalents. The reversal potential coincided with the expected Nernst sodium potential indicating that these patch currents are sodium selective, as are the sodium currents recorded from perfused squid giant axons.

Inactivation was incomplete in both the presence and absence of divalent ions. At the potential with maximum inward current (−10 to 0 mV), steady-state current accounted for 3–16% of the peak current. At the most positive potentials tested (+90 mV), steady-state current was more apparent, and amounted to 15–30% of the peak current. Similar results were observed with dialyzed axon under axial wire voltage clamp, but in that case steady-state current was greater, ~30% of the peak current at 0 mV.

Fig. 2 shows families of tail current records. In *A*, the external solution was 50 Mg, 10 Ca ASW and in *B*, for the same patch, the solution was changed to 546 Na. The sodium channels were activated by a brief pulse to the positive potential at which maximum peak current could

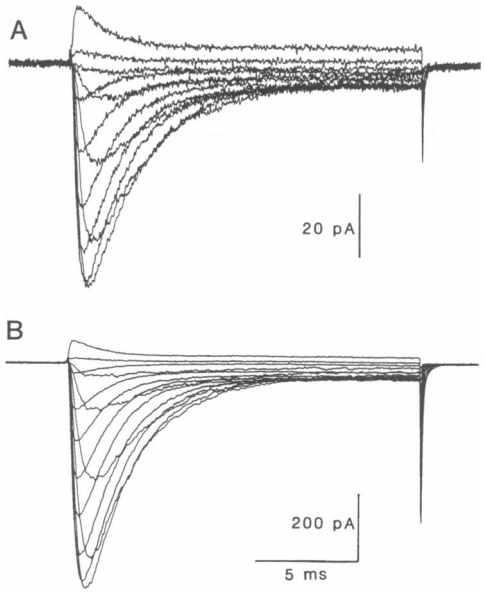

FIGURE 1 Macroscopic ionic currents with and without external divalents. Families of currents were recorded under different external ionic conditions for 18 ms depolarizing test pulses. (*A*) Currents from a patch bathed in 50 Mg, 10 Ca ASW for pulses to −37 to +73 mV, in 10-mV increments. The patch was held at −87 mV, and the test pulse was preceded by a 50-ms prepulse to −107 mV. Maximum peak current occurred for the pulse to +3 mV. (*B*) Currents for another patch with 546 Na as the external solution (no added divalent cations). Pulses were to voltages from −48 to +82 mV, in 10 mV increments, following a 50-ms prepulse to −108 mV. Holding potential was −98 mV. Maximum peak current was for the pulse to −8 mV. Currents represent averages of 16 cycles for *A* and eight cycles for *B*. Filter was 7 KHz.

be elicited, followed by postpulses to a series of hyperpolarizing and depolarizing potentials. The second peak present in tail currents for tail potentials more positive than the activating potential is due to further activation of the channels by the positive postpulse. Note that the amplitude of the current during the activating pulse increased substantially when the external solution was changed to 546 Na. More striking, however, was the difference in the magnitude of the tail currents, which in the presence of divalent cations did not increase as the potential was made more negative (Fig. 2*A*). In contrast, Fig. 2*B* shows that in the absence of divalent cations, the amplitude of the tail current increased in parallel with the magnitude of the negative postpulse (see also Fig. 3).

The differences in instantaneous tail current amplitudes is shown in more detail in Fig. 3 where the instantaneous current-voltage (I–V) relationships, together with single-channel current amplitudes, have been plotted for both conditions. The instantaneous I–V curves from different experiments were scaled using the

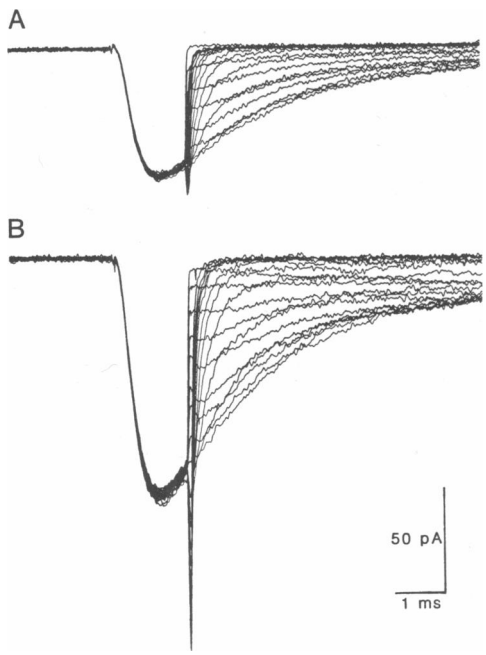

FIGURE 2 Macroscopic tail currents with and without external divalents. Families of tail currents were recorded following a 1.5-ms depolarizing pulse. (*A*) With 50 Mg, 10 Ca ASW as the external solution, tail currents were recorded from pulses to −107 to +63 mV, in 10 mV increments, following a depolarizing pulse to +3 mV. The holding potential was −87 mV, and the pulses were preceded by a 50-ms prepulse to −107 mV. (*B*) On the same patch, the external solution was then changed to 546 Na, and tail currents were recorded in the absence of external divalents. Tail currents are shown for postpulses to −107 to +73 mV, in 10-mV increments. The holding potential was −97 mV, prepulse was −107 mV for 50 ms, and the activating pulse was to −7 mV for 1.5 ms. Currents represent average of 24 cycles for *A* and 16 cycles for *B*. Filter was 7 KHz.

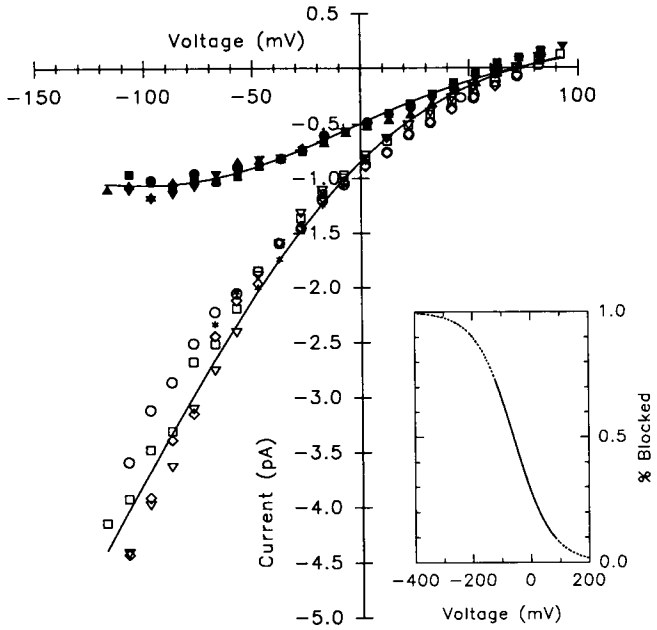

FIGURE 3 Instantaneous current-voltage-relationship. The instantaneous amplitude of the macroscopic tail current was obtained by fitting the tail currents with a single exponential, and extrapolating the fit to the beginning of the postpulse. Open symbols were obtained from patches in 546 Na external/150 Na internal solutions. Filled symbols were from patches in which the external solution was changed to 50 Mg, 10 Ca ASW. The curves were scaled by the amplitude of single-channel currents in the voltage range −50 mV to −30 mV. Average single-channel current amplitudes in the absence of divalents are shown as * symbols, and in the presence of 50 Mg, 10 Ca ASW as + symbols. The inset shows the percentage of current blocked in 50 Mg, 10 Ca ASW, with the solid line representing the voltage range over which the data were obtained. Fitted curves estimated block by divalent cations at a site 19% across the membrane field from the outside, with the midpoint at −58 mV.

amplitude of single-channel currents in the voltage range of −50 to −30 mV where the single-channel currents could be well resolved. Note that the current is plotted in units of pA, corresponding to single-channel amplitudes, although the instantaneous I–V relationships for macroscopic currents derive from experiments with peak currents at 0 mV in the range of 50–200 pA.

When the external solution was 50 Mg, 10 Ca ASW the instantaneous current saturated at −50 mV and it tended towards a negative slope conductance for more negative potentials. In contrast, the I–V curves recorded in 546 Na increased with hyperpolarization and became hyperlinear. A decrease in current amplitude with divalent cations has been observed in normal and batrachotoxin-modified sodium channels from a variety of tissues (Woodhull, 1973; Taylor et al., 1976; Mozhayeva et al., 1982; Yamamoto, et al., 1984; Worley et al., 1986; Moczydlowski et al., 1986; Green et al., 1987; Tanguy and Yeh, 1988; Ravindran et al., 1991). The interpretation of this phenomenon has been that the sodium channel is blocked by the divalent cations. As the membrane is hyperpolarized this block becomes more effective, indicating that the blocking site is within the membrane electrical field.

Current-voltage curves obtained in the absence of external divalent cations (546 Na external//50 Na internal) were fitted to the Goldman-Hodgkin-Katz (GHK) equation (Goldman, 1943; Hodgkin and Katz, 1949):

$$I = \left(\frac{P_{Na}F^2V}{RT}\right)\frac{[Na^+]_{in} - [Na^+]_{out}\exp(-FV/RT)}{1 - \exp(-FV/RT)}. \quad (2)$$

The estimated reversal potential of +73 mV deviated from +60 mV predicted from the sodium concentration gradient probably because the tail currents were small, and difficult to separate from the residual capacitative transient at positive potentials.

The I–V curve in the presence of 50 Mg, 10 Ca ASW

was fitted by a modified GHK equation allowing for block of the channel by external divalents, using the blocking model presented by Woodhull (1973). This model assumes that blocking ions bind to a single site on the channel located a fractional distance, d, across the membrane electrical field, and that the apparent dissociation constant of the blocker is an exponential function of voltage. The amount of current remaining in the presence of blocker, I_b, was described by the following equation:

$$I_b = I/[1 + [B]/K_d(0)\exp(zdFV/RT)], \quad (3)$$

where I is the current expected in the absence of blocker by Eq. 2, $[B]$ is the concentration of blocker, $K_d(0)$ is the apparent blocker dissociation constant at 0 mV, d is the fraction of the electrical field sensed by the divalent blocker, z is the valence of the blocking ion, V is the voltage, and R, T, and F have their usual meanings. The current-voltage curve was well-fitted by a voltage-dependent block that varied e-fold in 64 mV, which can be interpreted as binding of a divalent blocking ion at a site 19% of the electrical distance across the membrane field from the outside. If Ca^{2+} and Mg^{2+} are assumed to have similar affinities for the channel blocking site, the K_d for block at 0 mV was ~150 mM. The inset shows the block in 50 Mg, 10 Ca ASW expressed as a percentage of current blocked versus potential. The solid line indicates the range over which the data were obtained. The midpoint of the block, $V_{1/2}$, was at −58 mV.

Single-channel recordings

We explored the blocking effect of divalents as the cause of the nonlinear I–V relation of Fig. 3 by recording single-channel events in different external divalent cation concentrations. Fig. 4 shows single-channel events from continuous recordings at −48 mV for three different divalent concentrations. This membrane patch had a large number of sodium channels, permitting the recording of some single sodium channel openings in steady-state conditions from channels that returned from inactivation. The single-channel current transitions could be easily resolved when recordings were obtained in 546 Na, that is, in the absence of divalents (Fig. 4 *C*). When 10 mM Ca ASW was exchanged as the external medium (Fig. 4 *B*), the single-channel event size was approximately half of that recorded for the zero-divalent conditions. Similar current amplitudes were observed when 10 mM Mg^{2+} was included in the external solution instead of Ca^{2+} (not shown). Fig. 4 *A* shows single-channel recordings from the same patch in 50 Mg, 10 Ca ASW, and the events were barely resolved. These results indicate that divalent cations decreased the single sodium channel conductance presumably by entering and leaving the channel at very high rates producing a fast unresolved flicker block. At limited bandwidth the block appeared as a time-averaged decrease in the single-channel current.

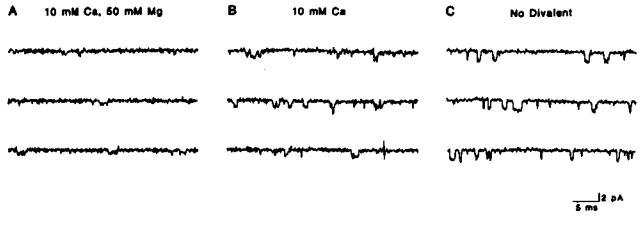

FIGURE 4 Single-channel currents. Steady-state recordings of single-channel events were obtained from a patch that contained a large number of channels. Representative continuous recordings are shown for a potential −48 mV when the external solution was either (*A*) 50 Mg, 10 Ca ASW; (*B*) 10 Ca ASW; or (*C*) 546 Na.

Voltage dependence of activation and inactivation

Fig. 5 *A* shows a plot of normalized peak I–V curves in 50 Mg, 10 Ca ASW (*filled symbols*) and in 546 Na (*open symbols*). The primary effect of adding divalent cations was to shift the voltage dependence of channel activation to more positive potentials. Thus, in 546 Na the currents were observed at potentials as negative as −60 mV, but in 50 Mg, 10 Ca ASW the currents activated only for potentials more depolarized than −40 mV. Similarly, the maximum peak current in the absence of divalents was at about −6 mV, and was near +6 mV with divalents. The shift of the peak I–V relationship was 12 mV.

The peak I–V curve (Fig. 5 *A*) contains contributions from the block of channels by divalents. To separate the channel blocking effect from effects on channel activation, we examined the number of channels open at the peak. The *F–V* curves of Fig. 5 *B*, showing the relative fraction of channels open at the peak current, were obtained by dividing the peak I–V data (Fig. 5 *A*) by the curves fitted to the instantaneous I–V (Fig. 3). The data then were normalized to the maximum fraction of channels open. The effect of external divalent cations also was to shift the F–V curve to depolarized potentials, by 9 mV, indicating that divalents caused a shift in peak channel open probability in addition to their blockage of channels. The block of channels by divalents accounted for the remaining 3 mV of shift in the peak current-voltage curve.

The minimum number of gating charges during channel activation can be estimated from the slope of the *F–V* curve at negative potentials (Almers, 1978). At the

foot of the activation curve the rate of rise of the *F–V* curve gave an e-fold change in 7–8 mV (Fig. 5 *C*). This indicates that the charge movement during channel opening is equivalent to a minimum of 3–4 gating charges moving across the membrane field. This value is comparable to the value of e-fold in 7 mV reported by Stimers et al. (1985) for pronase-treated axons, and is somewhat less voltage dependent than values found by others of e-fold in 4–7 mV (Hodgkin and Huxley, 1952*a*). When the nonlinearity of the instantaneous I–V has not been considered, the use of sodium conductance rather than proportion of channels may have led to slightly higher estimates of the number of gating charges. Inactivation of the current at negative potentials also can influence these estimates.

The voltage dependence of inactivation is shown as a prepulse inactivation curve (Hodgkin and Huxley, 1952*b*) in Fig. 6. Filled symbols were obtained in 50 Mg, 10 Ca ASW and open symbols in 546 Na. For comparison, data obtained from dialyzed axons with axial wire voltage clamp using 50 Mg, 10 Ca ASW are shown as half-filled symbols. As with the activation curve, the inactivation voltage dependence was shifted to more depolarized potentials when divalent cations were added. The magnitude of the shift was 13 mV.

The voltage dependence of the kinetics of channel deactivation is shown in Fig. 7. The plot represents the time constant, τ, of a single exponential fitted to tail current records such as the ones shown in Fig. 2. The time constant was voltage dependent and became faster as the membrane was hyperpolarized. The increased rate of channel closing at negative potentials is a characteristic of sodium channels that has been observed in many preparations. The effect of divalents again was to shift the curve of tail current time constant versus voltage to more depolarized potentials by 10 mV. The inset in Fig. 7 shows a detail of the plot for potential more negative than −60 mV. Notice that the time constants can be as short as 80 μs.

To ensure that low concentrations of calcium were not required for some aspect of channel gating, macroscopic sodium currents were recorded with buffering by EGTA on both sides of the membrane. Currents were recorded in 546 Na external//patch internal solution in which 5 mM EGTA had been added to the external solution. Time constants of activation, inactivation, and tail current deactivation were similar to those recorded in the nominal absence of divalent cations in the external solution (data not shown). Under these conditions we

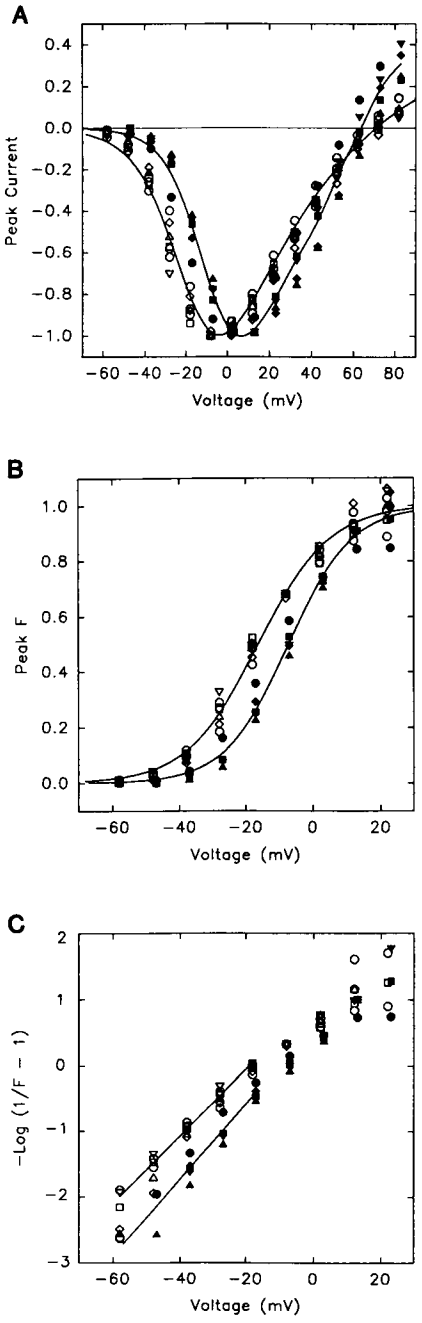

FIGURE 5 Peak current-voltage relationship and normalized fraction of channels open vs voltage. (*A*) The amplitude of the peak macroscopic current for depolarizing test pulses is plotted versus voltage. Data are from patches either in 50 Mg, 10 Ca ASW (*filled symbols*) or in 546 Na (*open symbols*). The currents were normalized to their maximum peak current. (*B*) The relative fraction of channels open versus voltage was obtained by dividing the peak current from (*A*) by the fitted instantaneous current from Fig. 3 for each voltage. Data for each ionic condition were fitted with a Boltzmann distribution, which gave midpoints of −16 mV (546 Na; *open symbols*) and −7 mV (50 Mg, 10 Ca ASW; *filled symbols*). (*C*) Plot of −Log (1/F−1) versus voltage showing the nearly exponential dependence of the peak fraction of channels open on the membrane voltage. The fitted slope of the line at the foot of the activation curve changed e-fold in 8.4 mV (546 Na; *open symbols*) or in 7.6 mV (50 Mg, 10 Ca ASW; *filled symbols*).

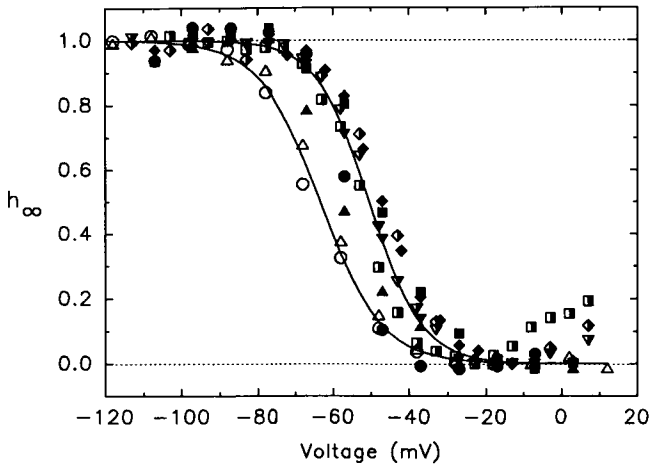

FIGURE 6 Prepulse inactivation versus voltage. Sodium current was inactivated by a 50-ms prepulse to the indicated voltage, followed by an activating test pulse to −8 or +3 mV to measure the amplitude of peak current remaining. Currents were measured from patches in the absence of external divalents using 546 Na external solution (*open symbols*), or in the presence of 50 Mg, 10 Ca ASW for both dialyzed whole axons (*half-filled symbols*) and patches (*filled symbols*). Steady-state current during the test pulse was subtracted before normalizing the currents to the current obtained from negative prepulses. The curve in 546 Na was fitted to a Boltzmann distribution, and had a midpoint at −63 mV and varied e-fold in 8 mV, while the curve in 50 Mg, 10 Ca ASW had a midpoint at −50 mV and varied e-fold in 7 mV.

estimate that buffered free calcium concentrations were <0.2 nM on both sides of the membrane if contaminating solution calcium concentrations were on the order of 20 μM.

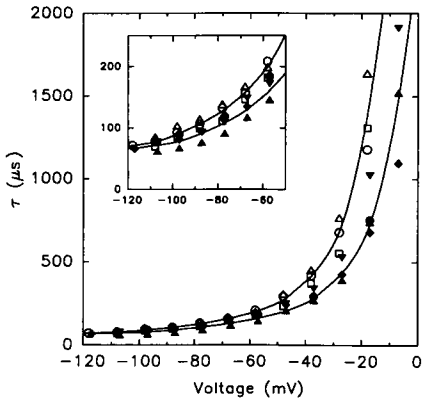

FIGURE 7 Tail current deactivation rate vs voltage. The rate of decline of tail currents was fitted to a single exponential curve. Open symbols were time constants from patches bathed in 546 Na external solution, and closed symbols from patches in 50 Mg, 10 Ca ASW. Curves through the data are shifted by 10 mV along the voltage-axis. The inset shows the negative voltage region on an expanded scale.

Gating currents

The high density of channels obtained in some of the patches from the cut-open axon made it possible to record gating currents. Fig. 8 shows recordings made in 10% sodium ASW for test pulses to −30, −10, and +20 mV from a prepulse potential of −110 mV. At the beginning of the pulse, the large outward transient current was ON gating current that was then masked by the inward sodium current. Upon repolarization of the membrane at the end of the pulse, the inward current transient was the sum of ionic sodium tail current and OFF gating current. These currents from patch recording show the same features of currents recorded in similar conditions in perfused axons with axial wire voltage clamp (Armstrong and Bezanilla, 1974). Gating currents are shown in more detail in Fig. 9 where the

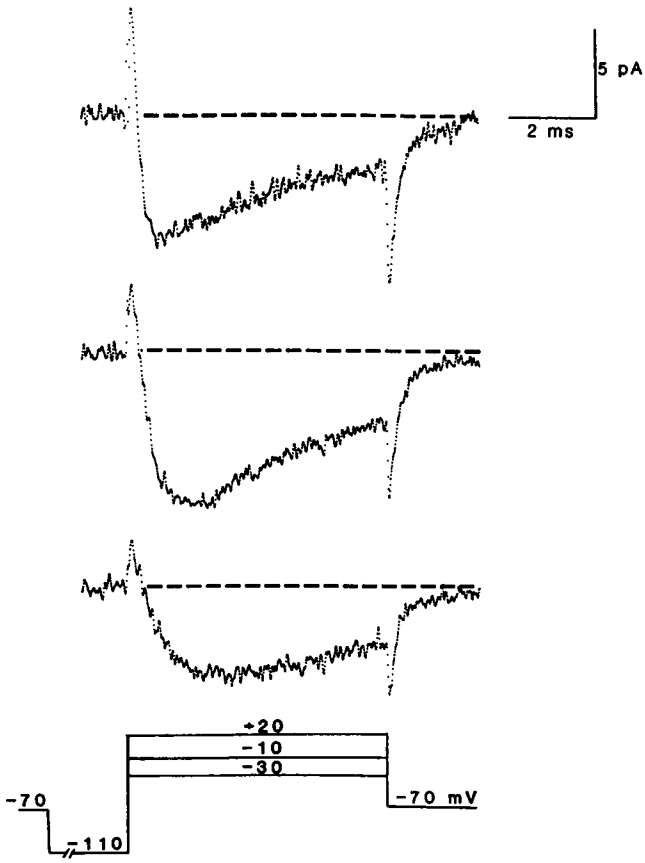

FIGURE 8 Patch recording of gating and ionic current. Macroscopic gating and ionic currents were recorded from a membrane patch for 6 ms voltage pulses to +20 mV (*upper record*), −10 mV (*middle record*), and −30 mV (*lower record*) from a prepulse potential of −110 mV. Solutions were 10% ASW external//patch gating internal. Currents were corrected for linear leakage and capacitative currents with the P/−4 procedure using a subtracting holding potential of −120 mV. Records represent the average of 10–20 cycles. Filter was 7.5 KHz.

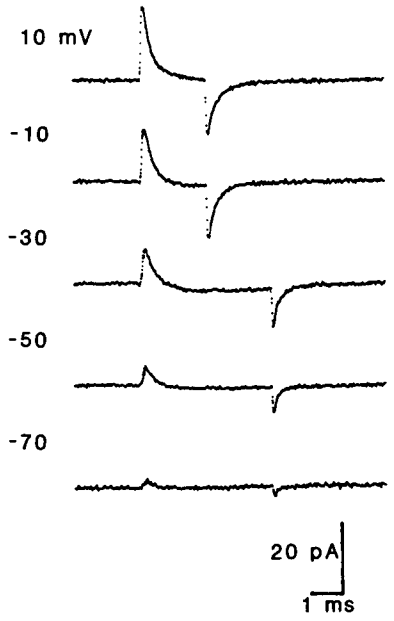

FIGURE 9 Patch gating currents. Gating currents were recorded from a membrane patch using the P/−4 method with a subtracting holding potential of −110 mV. Gating currents for 2 or 4-ms pulses to the indicated potential from a prepulse potential of −110 mV, and followed by a postpulse to −95 mV. Currents represent averages of 50–80 cycles. Filter was 7 KHz. Pipette diameter was 5 μm.

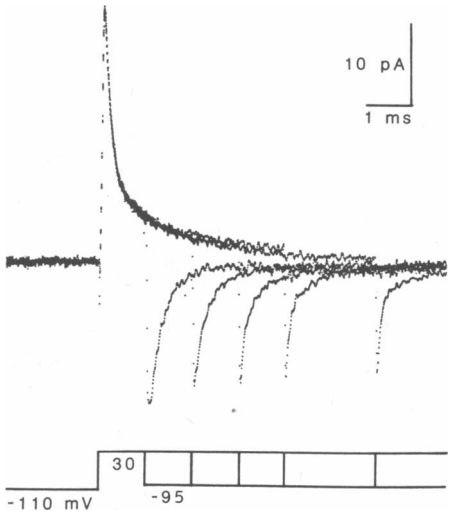

FIGURE 10 Charge immobilization in patch gating currents. Gating currents recorded from a membrane patch for test pulses of 1, 2, 3, 4, and 6 ms to +30 mV from a prepulse potential of −110 mV, and followed by a postpulse to −95 mV. The P/−4 method was used with a subtracting holding potential of −110 mV. Solutions contained no divalent cations, and were patch gating external//patch gating internal. Currents represent averages of 50–80 cycles. Filter was 7 KHz.

sodium current has been eliminated and the entire time course of the gating current can be observed without interference from the ionic current. In these records Na^+ in the medium was substituted with a combination of the relatively impermeant ions Cs^+ and tetramethyl ammonium, and with sucrose to eliminate ionic currents. The peak ON gating current increased with depolarization, and the time course of charge movement became faster such that the total charge, measured as the integral of the gating current, saturated with depolarization (see Fig. 11). The apparent rising phase observed in some of the ON gating currents is due to the limited recording bandwidth of 7 KHz.

The immobilization of gating charge, which has been shown to correspond to channel inactivation (Armstrong and Bezanilla, 1977) also can be measured in the patch gating current records. The ON gating charge that was moved upon depolarization could be recovered as OFF gating current during hyperpolarization. However, the OFF gating currents at the end of the pulse became progressively smaller as charge became immobilized with increasing durations of the depolarizing pulse as shown in Fig. 10. Also, notice that the OFF gating current appeared to have a single exponential time course for short duration pulses but it acquired a second slower component for longer durations. These results are in agreement with the description of charge immobilization demonstrated by Armstrong and Bezanilla (1977). The interpretation of the two components of the OFF gating current is that the fast one corresponds to the return of the nonimmobilized charge and the slower component is the return of the immobilized charge. As the postpulse potential is made more negative, the rate of the slow component becomes faster (Armstrong and Bezanilla, 1977), so it can be seen in records such as those of Fig. 10 to a postpulse potential of −95 mV.

Fig. 11 shows the relationship between the charge moved and the membrane potential (Q–V curve). In Fig. 11 *A* the Q–V curves were obtained from experiments with dialyzed axons under axial wire voltage clamp. We were able to perform a few experiments with only 1 or 4 mM Ca ASW as the external medium and obtain gating currents over a wide voltage range. The Q–V curve using 1 Ca ASW also was displaced to more negative potentials as compared to the one obtained with 50 Mg, 10 Ca ASW, in this case by 12 mV. This result indicates that the shift in the voltage dependence produced by divalent ions occurs at the level of the charge movement responsible for channel gating. In Fig. 11 *B*, a plot of the Q–V curve obtained from gating currents recorded in membrane patches in the absence of divalent cations is shown as a comparison. The signal-to-noise ratio of the data obtained in patch

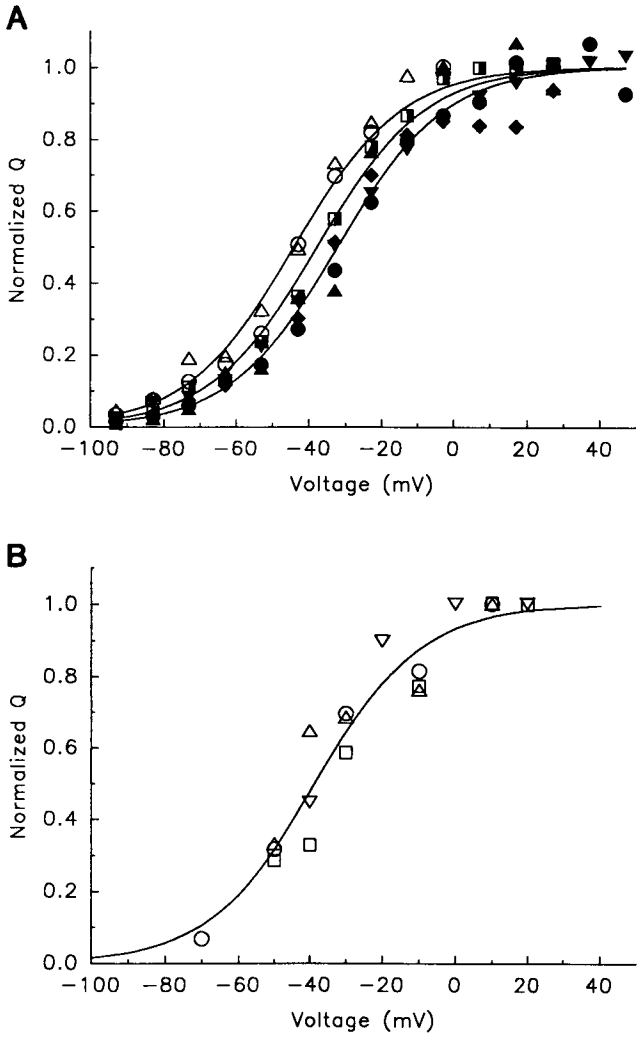

FIGURE 11 Gating current charge versus voltage relationships in whole axon and patches. (*A*) Integrated charge for ON gating current from dialyzed whole axon for pulses to the indicated voltages for axons bathed in 50 Mg, 10 Ca ASW (*filled symbols*), 4 Ca ASW (*half-filled symbols*), and 1 Ca ASW (*open symbols*). Data were fitted with a Boltzmann distribution with a slope increasing e-fold in 15 mV (1.6 electronic charges) and midpoints at −32 mV, −38 mV, and −44 mV respectively. Data are from two axons, with data in 50 Mg, 10 Ca ASW both before and after recordings in the lower divalent solutions. (*B*) Integrated ON gating current for patches in the absence of divalent cations. Solutions were patch gating external//patch gating internal. Fitted Boltzmann distribution changed e-fold in 15 mV, with a mid-point at −39 mV.

experiments is much lower than the data obtained with whole axon and consequently the *Q–V* curve shows more scatter. It is clear, however, that the results of the patch experiment are in general agreement with the data recorded from dialyzed axons.

The effects of changes of external solution on the gating and ionic currents were reversible. The *Q–V* curves of Fig. 10*A* were obtained from two axons in which the measurements in 50 Mg, 10 Ca ASW were made both before and after the measurements in low divalent ASW. The agreement between the values shows that the divalent-induced voltage shifts are temporary effects due to the presence or absence of the external divalents.

Long-term changes were observed in some experiments using dialyzed whole axons in the rising phase of the ON gating currents. Stimers et al. (1987) have shown that the brief rising phase often recorded in the ON gating currents is a recording artifact due to uncompensated series resistance in the Frankenhaeuser-Hodgkin space surrounding the axon. They found that the rising phase could be eliminated by bathing the axon in a hyperosmotic external solution. We find that in axons that displayed a rising phase in 50 Mg, 10 Ca ASW, that rising phase was eliminated or greatly reduced by bathing the axon briefly in 4 Ca ASW or 1 Ca ASW before returning it to 50 Mg, 10 Ca ASW. It is possible that low divalent ASW disrupted the association of the axon with the surrounding connective tissue. The increase in leakiness of the whole axon with long incubations in low divalent ASW also may follow as a consequence.

DISCUSSION

In this paper we have shown single sodium channel currents, macroscopic sodium currents and sodium gating currents all obtained with patch clamp methods. It is of clear advantage to be able to record all the electrical expressions of channel activity in the same preparation and with the same technique because modeling of channel gating will require all these experimental results from the same preparation and in the same conditions. The currents obtained by patch recordings offer several advantages, including the ability to resolve single-channel currents, and the opportunity to record macroscopic currents in a variety of solutions of varying divalent ion concentration as well as wide ranges of osmotic strength. Macroscopic patch recordings from the giant axon allow for fast, reliable voltage clamping of ionic currents without the large capacitative transient associated with whole-cell recordings from isolated cells, and for that reason, measurement of gating current also has been possible. However, the signal-to-noise ratios of macroscopic and gating current recordings were not as high as those obtained in whole axon and for this reason we have made comparisons of results obtained in both types of preparations.

Patch recordings as compared to whole axon recordings

The macroscopic currents recorded with patch pipettes compare very well with currents recorded in perfused and dialyzed axons, both in voltage dependence and time course. The general features of gating currents were in good agreement with recordings made in whole axon: the voltage dependence of the Q–V curves were similar and the immobilization of the charge also was very similar. The conclusion is that the sodium and gating currents recorded in the patch are comparable with the wealth of information available in the whole axon, and by extrapolation, the single-channel currents recorded in the patch also are comparable.

The difference we have observed between recordings with patch pipettes and with perfused and dialyzed axons is the amount of steady-state ionic current at high depolarizations. In the case of the whole axon, inactivation tended to be less complete at higher depolarizations and this tendency was less marked in patch recordings. We speculate that this was due to the difference in internal cations in the two recording situations.

We have paid special attention to the effect of calcium and magnesium on the sodium current because we found that the amplitude of single-channel records was reduced drastically when the divalent cation concentration was increased in the external medium. In particular, under the conditions of 50 Mg, 10 Ca ASW the single-channel events almost were unresolvable. For this reason, we chose to study single channel currents in the absence of divalent cations (see next paper). Considering that most of the data available from macroscopic currents and gating currents obtained in whole axon has come from experiments using high divalent concentrations, we have studied the effect of divalent cations on the activation and inactivation processes in macroscopic current under patch recordings. One important advantage of patch recordings over whole axon recordings is the possibility of acquiring data under conditions of zero divalent cations. In whole axons, either dialyzed or perfused under voltage clamp conditions, it has not been possible to perform experiments in the total absence of divalent cations because the leakage current was found to increase rapidly to intolerable levels. This might be due to disruption of the structural relationship between the axon and the Schwann cells, causing an increase in leakage. In contrast, under patch clamp conditions with the cut-open axon we found that seals could be made easily in the absence of divalent cations and currents could be recorded for several hours in the same patch. This has allowed us to compare the channel properties with and without divalent cations. We found that external calcium or magnesium blocked the open channel and shifted the voltage gating characteristics to more positive potentials.

Divalent cations block the open sodium channel

Single-channel current data showed that external divalent cations interfere with the normal conduction of sodium through the open channel (Fig. 4). The blockage appears to be extremely fast because rapid closings of the current were not visible and instead a time-averaged decrease of the single-channel current was observed. We found it necessary to reduce external divalents to obtain well resolved single-channel currents because considerable blockage occurs in the voltage region of -60 to 0 mV in which single channels currents usually can be best resolved due to the sodium driving force.

The blocking effect of calcium and magnesium was reported in perfused axons (Taylor et al., 1976; Tanguy and Yeh, 1988), in neuroblastoma cells (Yamamoto, et al., 1984), frog node of Ranvier (Woodhull, 1973) and in batrachotoxin-modified sodium channels from amphibian nerve (Mozhayeva et al., 1982), mammalian brain (Worley et al., 1986; Green et al., 1987) and muscle (Moczydlowski et al., 1986; Ravindran et al., 1991). The blockage is voltage dependent (Figs. 2 and 3) and it is enhanced with hyperpolarization, as expected if the binding site for divalent cations is within the membrane field. The estimated electrical distance of the binding site within the membrane field (0.19 from the outside) is similar to that obtained for Ca^{2+} block in a variety of tissues and species, suggesting a conserved structural feature of the sodium channel throughout evolution.

Voltage-dependent divalent block of the sodium channel was most pronounced at negative potentials. At membrane potentials near threshold (~ -60 mV), the channel is $\sim 50\%$ blocked by physiological concentrations of divalent cations. Relief of open-channel block can explain some of the increased excitability reported for axons bathed in the absence of extracellular divalents (Frankenhaeuser, 1957; Frankenhaeuser and Hodgkin, 1957).

Divalent cations shift the voltage dependence of gating

External divalent cations showed effects on channel gating in addition to open-channel blockage. Blockage of the current, for example, does not explain the shift of the peak I–V curves (Fig. 5 *A*) because the main effects of the nonlinearity of conductance due to channel block occur at more negative potentials than the increase in conductance due to channel opening. Note that the F–V curve (Fig. 5 *B*), which is corrected for effects of channel

block, is shifted nearly as much as the peak I–V curve by external divalents (Fig. 5 *A*).

The voltage dependences of activation and inactivation as well as the voltage dependence of the deactivation kinetics were shifted towards depolarized potentials by divalent cations (see Figs. 5, 6, and 7). The magnitude of the shift was similar for all processes examined indicating that the effect is mediated through a process analogous to surface charge screening. In addition, the *Q–V* curves were shifted to the right by the same amount by divalents. This is consistent with the screening of charge and a change in the local potential seen by the voltage sensors mediating channel activation, deactivation and inactivation. The results are consistent with a simple shift of the voltage dependence as if there were an extra potential added to the bulk potential sensed by the gating machinery. Similar shifts induced by divalent cations have been reported for sodium channels in frog nerve (Hille, 1968; Hille et al., 1975) and muscle (Campbell and Hille, 1976; Hahin and Campbell, 1983), and batrachotoxin-activated sodium channels in planar lipid bilayers (Cukierman et al., 1988). Depolarizing shifts in the conductance-voltage relationship were originally described in the squid by Frankenhaeuser and Hodgkin (1957) who suggested that binding of divalents to negative charges on the membrane could alter the electrical field sensed by the channel gate. Studies in bilayers of varying lipid composition have shown that contributions from the electrostatic potential due to charges on both the channel protein and the membrane lipid are consistent with shifts in channel activation by calcium (Cukierman et al., 1988).

Calcium ions are not required for channel closing

An alternative proposal for the effect of divalent cations has been that the binding of divalents to part of the gating apparatus is a fundamental aspect of channel gating. It has been suggested that external Ca^{2+} is required for closing potassium channels (Armstrong and Matteson, 1986; Armstrong and Miller, 1990) as well as sodium channel (Armstrong and Bamrungphol, 1987). In the case of sodium channels, this suggestion was based on the increase in tail current time constants when external Ca^{2+} concentration was decreased <5 mM in perfused squid giant axons under axial wire voltage clamp. Using patch recording techniques, in which we were able to voltage clamp and record sodium currents in subnanomolar external and internal Ca^{2+}, we show that calcium ions are not required for channel closing. We also found that sodium ionic and gating currents behaved normally in dialyzed whole axons under axial wire voltage clamp when Ca^{2+} was decreased to 1 mM. However further decreases caused an increase in leak current and an inability to maintain the whole axon under voltage clamp. Our results are consistent with the idea that extracellular divalent cations cause a ~ 10 mV shift in the gating kinetics of the sodium channel due to charge screening, and an outward rectification of single-channel or instantaneous tail current due to open channel block. There was no evidence for additional effects of Ca^{2+} on the gating process.

All the single channel records presented and analyzed in the next paper were obtained in the absence of divalents and the analysis of the combined results of single, macroscopic and gating currents were done assuming that data with divalents can be combined with data without divalents by simply allowing a shift in the voltage dependence.

We thank Drs. Ana Maria Correa, Richard Horn and Eduardo Perozo for critically reading the manuscript.

This work was supported by National Institutes of Health grants GM 30376 and HL 41656.

Received for publication 11 June 1991 and in final form 21 August 1991.

REFERENCES

Almers, W. 1978. Gating currents and charge movements in excitable membranes. *Rev. Physiol. Biochem. Pharmacol.* 82:6–190.

Armstrong, C. M., and W. Bamrungphol. 1987. The effects of low external calcium concentration on sodium channels closing kinetics in squid giant axons. *Biophys. J.* 51:9a.

Armstrong, C. M., and F. Bezanilla. 1974. Charge movement associated with the opening and closing of the activation gates of the Na channels. *J. Gen. Physiol.* 63:533–552.

Armstrong, C. M., and F. Bezanilla. 1977. Inactivation of the sodium channel. II. Gating current experiments. *J. Gen. Physiol.* 70:567–590.

Armstrong, C. M., and D. R. Matteson. 1986. The role of calcium ions in the closing of K channels. *J. Gen. Physiol.* 87:817–832.

Armstrong, C. M., and C. Miller. 1990. Do voltage-dependent K^+ channels require Ca^{2+}? A critical test employing a heterologous expression system. *Proc. Natl. Acad. Sci. USA* 87:7579–7582.

Bezanilla, F. 1987. Single sodium channels from the squid giant axon. *Biophys. J.* 52:1087–1090.

Bezanilla, F., and C. M. Armstrong. 1977. Inactivation of the sodium channel. I. Sodium current experiments. *J. Gen. Physiol.* 70:549–566.

Bezanilla, F., R. E. Taylor, and J. M. Fernandez. 1982. Distribution and kinetics of membrane dielectric polarization. I. Long-term inactivation of gating currents. *J. Gen. Physiol.* 79:21–40.

Bezanilla, F., and C. Vandenberg. 1990. The cut-open axon technique. In: *Squid as Experimental Animals.* D. L. Gilbert, W. J. Adelman, Jr., and J. M. Arnold, eds. Plenum Press. pp. 153–159.

Brinley, F. J., and L. J. Mullins. 1967. Sodium extrusion by internally dialyzed squid axons. *J. Gen. Physiol.* 50:2303–2331.

Campbell, D. T., and B. Hille. 1976. Kinetic and pharmacological properties of the sodium channel of frog skeletal muscle. *J. Gen. Physiol.* 67:309–323.

Cukierman, S., W. C. Zinkand, R. J. French, and B. K. Krueger. 1988. Effects of membrane surface charge and calcium on the gating of rat brain sodium channels in planar bilayers. *J. Gen. Physiol.* 92:431–447.

Dipolo, R., F. Bezanilla, C. Caputo, and H. Rojas. 1985. Voltage dependence of the Na/Ca exchange in voltage-clamped, dialyzed squid axons. *J. Gen. Physiol.* 86:457–478.

Frankenhaeuser, B. 1957. The effect of calcium on the myelinated nerve fibre. *J. Physiol. (Lond.)* 137:245–260.

Frankenhaeuser, B., and A. L. Hodgkin. 1957. The action of calcium on the electrical properties of squid axons. *J. Physiol. (Lond.)* 137:218–244.

Goldman, D. E. 1943. Potential, impedance, and rectification in membranes. *J. Gen. Physiol.* 27:37–60.

Green, W. N., L. B. Weiss, and O. S. Andersen. 1987. Batrachotoxin-modified sodium channels in planar lipid bilayers. *J. Gen. Physiol.* 89:841–872.

Hahin, R., and D. T. Campbell. 1983. Simple shifts in the voltage dependence of sodium channel gating caused by divalent cations. *J. Gen. Physiol.* 82:785–805.

Hamill, O. P., A. Marty, E. Neher, B. Sakmann, and F. J. Sigworth. 1981. Improved patch-clamp techniques for high-resolution current recording from cells and cell-free membrane patches. *Pflugers Arch.* 391:85–100.

Hille, B. 1968. Charges and potentials at the nerve surface. Divalent ions and pH. *J. Gen. Physiol.* 51:221–236.

Hille, B., A. M. Woodhull, and B. I. Shapiro. 1975. Negative surface charge near sodium channels of nerve: Divalent ions, monovalent ions, and pH. *Phil. Trans. Royal Soc. Lond. B* 270:301–318.

Hodgkin, A. L., and A. F. Huxley. 1952*a*. A quantitative description of the membrane current and its application to conduction and excitation in nerve. *J. Physiol. (Lond.)* 117:500–544.

Hodgkin, A. L. and A. F. Huxley. 1952*b*. Currents carried by sodium and potassium ions through the membrane of the giant axon of *Loligo*. *J. Physiol. (Lond.)* 116:449–472.

Hodgkin, A. L., and B. Katz. 1949. The effect of sodium ions on the electrical activity of the giant axon of the squid. *J. Physiol. (Lond.)* 128:61–88.

Llano, I., C. K. Webb, and F. Bezanilla. 1988. Potassium conductance of the squid giant axon. Single-channel studies. *J. Gen. Physiol.* 92:179–196.

Moczydlowski, E., A. Uehara, X. Guo, and J. Heiny. 1986. Isochannels and blocking modes of voltage-dependent sodium channels. *Ann. New York Acad. Sci.* 479:269–292.

Mozhayeva, G. N., A. P. Naumov, and B. I. Khodorov. 1982. Potential dependent blockage of batrachotoxin-modified sodium channels in frog node of Ranvier by calcium ions. *Gen. Physiol. Biophys.* 1:281–282.

Ravindran, A., Schild, L., and E. Moczydlowski. 1991. Divalent cation selectivity for external block of voltage-dependent Na^+ channels prolonged by batrachotoxin. *J. Gen. Physiol.* 97:89–115.

Stimers, J. R., F. Bezanilla, and R. E. Taylor. 1985. Sodium channel activation in the squid giant axon. Steady state properties. *J. Gen. Physiol.* 85:65–82.

Stimers, J. R., F. Bezanilla, and R. E. Taylor. 1987. Sodium channel gating currents. Origin of the rising phase. *J. Gen. Physiol.* 89:521–540.

Tanguy, J., and J. Z. Yeh. 1988. Divalent cation block of normal and BTX-modified sodium channels in squid axons. *Biophys. J.* 53:229a.

Taylor, R. E., C. M. Armstrong, and F. Bezanilla. 1976. Block of sodium channels by external calcium ions. *Biophys. J.* 16:27a.

Vandenberg, C. A., and F. Bezanilla. 1988. Single-channel, macroscopic and gating currents from Na channels in squid giant axon. *Biophys. J.* 53:226a.

Vandenberg, C. A., and F. Bezanilla. 1990. Modeling Na channels in squid giant axon from single-channel, macroscopic and gating currents. *Biophys. J.* 57:296a.

Vandenberg, C. A. and F. Bezanilla. 1991. A sodium channel gating model based on single-channel, macroscopic ionic and gating currents in the squid giant axon. *Biophys. J.* 60:1511–1533.

Woodhull, A. M. 1973. Ionic blockage of sodium channels in nerve. *J. Gen. Physiol.* 61:687–708.

Worley, J. F., R. J. French and B. K. Krueger. 1986. Trimethyloxonium modification of single batrachotoxin-activated sodium channels in planar bilayers. Changes in unit conductance and in block by saxitoxin and calcium. *J. Gen. Physiol.* 87:327–349.

Yamamoto, D., J. Z. Yeh, and T. Narahashi. 1984. Voltage-dependent calcium block of normal and tetramethrin-modified single sodium channels. *Biophys. J.* 45:337–344.